

Nonperipherally Octa(butyloxy)-Substituted Phthalocyanine Derivatives with Good Crystallinity: Effects of Metal–Ligand Coordination on the Molecular Structure, Internal Structure, and Dimensions of Self-Assembled Nanostructures

Yingning Gao,^[a, b] Yanli Chen,^[c] Renjie Li,^[b] Yongzhong Bian,^[a] Xiyu Li,^[b] and Jianzhuang Jiang^{*[a, b]}

Abstract: To investigate the effects of metal–ligand coordination on the molecular structure, internal structure, dimensions, and morphology of self-assembled nanostructures, two nonperipherally octa(alkoxyl)-substituted phthalocyanine compounds with good crystallinity, namely, metal-free 1,4,8,11,15,18,22,25-octa(butyloxy)-phthalocyanine $\text{H}_2\text{Pc}(\alpha\text{-OC}_4\text{H}_9)_8$ (**1**) and its lead complex $\text{Pb}[\text{Pc}(\alpha\text{-OC}_4\text{H}_9)_8]$ (**2**), were synthesized. Single-crystal X-ray diffraction analysis revealed the distorted molecular structure of metal-free phthalocyanine with a saddle conformation. In the crystal of **2**, two monomeric molecules are linked by coordination of the Pb atom of one molecule with an aza-nitrogen atom and its two neighboring oxygen atoms from the butyloxy substituents of another molecule, thereby forming a Pb-connected pseudo-double-decker supramolecular structure with a domed conformation for the phthalocyanine ligand. The self-assembling properties of **1** and **2** in the absence and presence of sodium ions were comparatively investigated by scanning electronic microscopy (SEM),

spectroscopy, and X-ray diffraction techniques. Intermolecular π – π interactions between metal-free phthalocyanine molecules led to the formation of nanoribbons several micrometers in length and with an average width of approximately 100 nm, whereas the phthalocyaninato lead complex self-assembles into nanostructures also with the ribbon morphology and micrometer length but with a different average width of approximately 150 nm depending on the π – π interactions between neighboring Pb-connected pseudo-double-decker building blocks. This revealed the effect of the molecular structure (conformation) associated with metal–ligand ($\text{Pb-N}_{\text{isoindole}}$, Pb-N_{aza} , and $\text{Pb-O}_{\text{butyloxy}}$) coordination on the dimensions of the nanostructures. In the presence of Na^+ , additional metal–ligand (Na-N_{aza} and $\text{Na-O}_{\text{butyloxy}}$) coordination bonds formed between sodium atoms and aza-nitro-

gen atoms and the neighboring butyloxy oxygen atoms of two metal-free phthalocyanine molecules cooperate with the intrinsic intermolecular π – π interactions, thereby resulting in an Na-connected pseudo-double-decker building block with a twisted structure for the phthalocyanine ligand, which self-assembles into twisted nanoribbons with an average width of approximately 50 nm depending on the intertetrapyrrole π – π interaction. This is evidenced by the X-ray diffraction analysis results for the resulting aggregates. Twisted nanoribbons with an average width of approximately 100 nm were also formed from the lead coordination compound **2** in the presence of Na^+ with a Pb-connected pseudo-double-decker as the building block due to the formation of metal–ligand (Na-N_{aza} and $\text{Na-O}_{\text{butyloxy}}$) coordination bonds between additionally introduced sodium ions and two phthalocyanine ligands of neighboring pseudo-double-decker building blocks.


Keywords: coordination bonds • nanostructures • phthalocyanine • pi interactions • self-assembly

[a] Y. Gao, Dr. Y. Bian, Prof. J. Jiang
Department of Chemistry
University of Science and Technology Beijing
Beijing 100083 (China)
Fax: (+86) 10-6233-2462
E-mail: jianzhuang@ustb.edu.cn

[b] Y. Gao, R. Li, Prof. X. Li, Prof. J. Jiang
Department of Chemistry
Shandong University

Jinan 250100 (China)
Fax: (+86) 531-8856-5211
E-mail: jzjiang@sdu.edu.cn

[c] Prof. Y. Chen
Department of Chemistry
University of Jinan
Jinan 250100 (China)

 Supporting information for this article is available on the WWW under <http://dx.doi.org/10.1002/chem.200901722>.

Introduction

A major ambition in the field of nanoscience and nanotechnology is the preparation of nanostructures with controllable dimensions and morphology, and in particular, a high molecular ordering nature due to the significant effects of molecular ordering and the dimensions of nanostructures on nano-device performance and size.^[1–6] A wide range of nanostructures with different morphology have been fabricated from the self-assembly processes of various functional molecular materials that are dependent on noncovalent interactions.^[7–17] However, most probably due to the short range and relatively low molecular ordering nature of the self-assembled nanostructures associated with the limited dimension(s) in some direction(s) and the rapidly increasing speed of self-assembled nanostructures that enable them to form before reaching their thermodynamic equilibrium, few self-assembled molecular nanostructures are able to provide enough internal structural information, especially through X-ray diffraction analysis. Examination of a large number of self-assembled nanostructures reported thus far indicates that self-assembled nanostructures of molecular materials seldom exhibit rich refraction peak(s) in their X-ray diffraction (XRD) patterns.^[18–25] Quite a significant fraction of self-assembled nanostructures do not even give any XRD refraction peak.^[26–30] As a result, most self-assembled organic nanostructures reported thus far were usually characterized only in terms of their morphology and dimension by means of various electronic microscopic techniques but without giving enough internal structural information due to the small amount of XRD data revealed. For the purpose of fabricating organic nanostructures with controllable morphology, dimensions, and in particular, a high molecular ordering nature, which allow for the investigation of the internal structure through XRD analysis, molecular materials with good crystallinity associated with a regular molecular structure and suitable intermolecular interactions are expected to play an important role in this regard.

Since their first synthesis early last century, phthalocyanines, which typically possess a large conjugated molecular electronic structure, have been an important industrial commodity used as inks, dyestuffs, and catalysts for sulfur effluent removal.^[31] In particular, bis- and tris(phthalocyaninato) metal complexes with sandwich-type double- and triple-decker structures have been recently emerging as advanced molecular materials with great potential applications in the fields of sensors, molecular electronics, molecular magnets, organic field-effect transistors, and molecular information-storage materials.^[32–36] For the fabrication of phthalocyanine-based nanodevices with diverse applications, the self-assembly of functional phthalocyanine derivatives into well-defined nanostructures has attracted increasing research interest in recent years.^[37–43] In addition, organized films of octa(alkoxy)-substituted phthalocyanines were prepared by means of the Langmuir–Blodgett (LB) technique.^[44] The dominant π – π interaction among the phthalocyanine molecules usually leads to one-dimensional nanostructures. For

example, nanoribbons and nanowires were obtained from unsubstituted phthalocyaninato (Pc)–metal complexes MPc (M = Co, Cu, Fe, Ni, Zn).^[41] Molecules of metal-free peripherally substituted octa(octyloxy)phthalocyanine H₂Pc-(OC₈H₁₇)₈ self-assemble into nanofibers.^[42] However, to the best of our knowledge, octa-substituted phthalocyanine derivatives with eight functional substituents incorporated onto the nonperipheral positions of the phthalocyanine ring have never been employed to self-assemble into nanostructures. It is worth noting that during the preparation of the present manuscript, Zhang and co-workers reported SEM images of 1,4,8,11,15,18,22,25-octa(butyloxy)phthalocyaninato copper one-dimensional microwire at the silicon, glass, and indium–tin oxide (ITO) surface obtained by solvent evaporation.^[45]

Among various kinds of phthalocyanine derivatives, nonperipherally octa(alkoxy)-substituted phthalocyanine compounds are of good crystallinity,^[46–48] they are therefore expected to induce high molecular ordering in their self-assembled nanostructures, thus allowing for the investigation of their internal structure by means of X-ray diffraction techniques. This, in combination with their available crystal and molecular structure revealed by single-crystal X-ray diffraction analysis, should render it possible to investigate the formation mechanism as well as the molecular packing mode of self-assembled nanostructures of corresponding compounds in a confirmed manner.

Results and Discussion

Synthesis and characterization: Phthalocyanines typically have a large conjugated molecular electronic structure. The dominant intermolecular π – π interactions among the phthalocyanine molecules usually lead to one-dimensional nanostructures. Tuning the intermolecular interaction of such a tetrapyrrole derivative towards high-molecular-ordered self-assembled nanostructures can therefore be reached by incorporating functional groups (actually, additional noncovalent interactions) onto the phthalocyanine ring. Previous studies revealed that incorporation of oxygen atoms at the nonperipheral positions of the phthalocyanine ring renders it possible to form coordination bonds with additionally introduced sodium ions with the help of aza-nitrogen atoms.^[47] This provides an effective way to tune the intermolecular interaction of nonperipherally octa(alkoxy)-substituted phthalocyanine derivatives through metal–ligand coordination bonding interactions. Nevertheless, among various kinds of known phthalocyanine derivatives, nonperipherally octa(alkoxy)-substituted phthalocyanine compounds have been revealed to possess good crystallinity due to their regular molecular structure and suitable intermolecular interactions^[46–48] and are therefore also expected to induce high molecular ordering in their self-assembled nanostructures, thus allowing investigation of their internal structure through X-ray diffraction analysis. As a result, metal-free 1,4,8,11,15,18,22,25-octa(butyloxy)phthalocyanine H₂Pc(α -OC₄H₉)₈ (**1**) was pre-

pared according to the published procedure,^[49,50] and its self-assembly behavior was comparatively studied in the absence and presence of sodium ions. In addition, with an idea about the close relationship between the molecular structure and dimensions of self-assembled nanostructures in mind, the lead ion was introduced into the phthalocyanine central hole to induce the change from the saddle conformation for metal-free phthalocyanine **1** to a domed one for the phthalocyaninato lead complex.^[51,52] Both the single-crystal structure and the self-assembled nanostructure of the resulting complex $\text{Pb}[\text{Pc}(\alpha\text{-OC}_4\text{H}_9)_8]$ (**2**) were also comparatively studied to reveal the effects of metal–ligand coordination on the internal structure, morphology, and dimensions of self-assembled nanostructures.

The phthalocyaninato lead complex **2** was synthesized in good yield from the reaction between metal-free phthalocyanine and $\text{Pb}(\text{OAc})\cdot 3\text{H}_2\text{O}$ in DMF. Satisfactory elemental analysis results were obtained for the newly prepared phthalocyaninato lead complex after repeated column chromatographic purification and recrystallization. The MALDI-TOF mass spectrum of **2** showed an intense signal for the molecular ion $[M+H]^+$. Compound **2** was also characterized by means of a range of spectroscopic methods. The ^1H NMR spectrum of this compound was recorded in CDCl_3 at room temperature. All the signals can be readily assigned (Figure S1 in the Supporting Information).

X-ray single-crystal structure: The crystal and molecular structures of the phthalocyanine derivatives **1** and **2** were determined by X-ray diffraction analyses. Single crystals of **1** and **2** suitable for X-ray diffraction analysis were obtained by slow diffusion of MeOH into a solution of **1** or **2** in CHCl_3 . Compound **1** crystallizes in the triclinic system with a $P\bar{1}$ space group with two molecules per unit cell (Figure S2A in the Supporting Information). In contrast, compound **2** crystallizes in the monoclinic system with a $P2_1/c$ space group with four molecules per unit cell (Figure S2B).

Figure 1 displays the molecular structure of **1**. The steric hindrance arising from the eight nonperipheral butyloxy groups induces a distorted molecular structure with a saddle conformation employed by the metal-free phthalocyanine **1**, Figure 1B. The individual isoindole ring is tilted alternately up and down from the $\text{N}(\text{isoindole})_4$ mean plane. The dihedral angles formed between the isoindole units and the $\text{N}(\text{isoindole})_4$ plane are 14.58, 16.78, 18.27, and 18.83°, respectively. Despite the deformed molecular structure with a saddle conformation adopted by metal-free phthalocyanine, effective π – π interactions exist between the neighboring phthalocyanine molecules due to the short distance between two overlapped isoindole sections of the neighboring phthalocyanine molecules with a separation of 3.351 and 4.019 Å in an alternating manner (Figure 1C). As a consequence, the separation between neighboring phthalocyanine molecules in terms of the $\text{N}(\text{isoindole})_4$ plane in the crystal of metal-free phthalocyanine is also in an alternating manner, changing from 4.848 to 4.961 Å (Figure 1C).

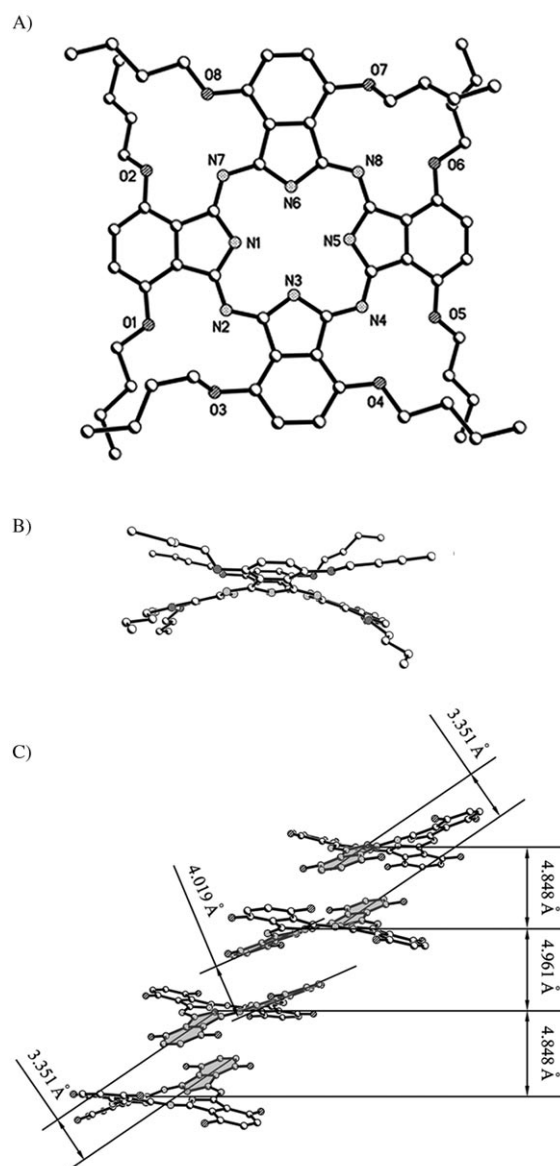


Figure 1. A) Top view and B) side view of the molecular structure of $\text{H}_2\text{Pc}(\alpha\text{-OC}_4\text{H}_9)_8$ (**1**) together with C) the crystal-packing mode. Hydrogen atoms in all the parts and alkoxy side chains in C are omitted for clarity.

The molecular structure of the phthalocyaninato lead complex **2** is shown in Figure 2. This represents the first structurally characterized phthalocyaninato lead complex with eight alkoxy groups at the nonperipheral positions. As shown in Figure 2C, two molecules of **2** are bound to each other through a $\text{Pb}-\eta^3\text{-Pc}(\alpha\text{-OC}_4\text{H}_9)_8$ coordination. The lead atom of one molecule binds to an aza-nitrogen atom and its two neighboring oxygen atoms from two butyloxy groups of another molecule, thus forming a Pb-connected pseudo-double-decker supramolecular structure. The ring-to-ring separation of these two virtually parallel $\text{N}(\text{isoindole})_4$ mean planes of $\text{Pc}(\alpha\text{-OC}_4\text{H}_9)_8$ is 2.880 Å (Figure 2C). This value is comparable with that found in the corresponding double-decker complex of $\text{EuH}[\text{Pc}(\alpha\text{-OC}_4\text{H}_9)_8]_2$ (2.89 Å),^[48] thereby

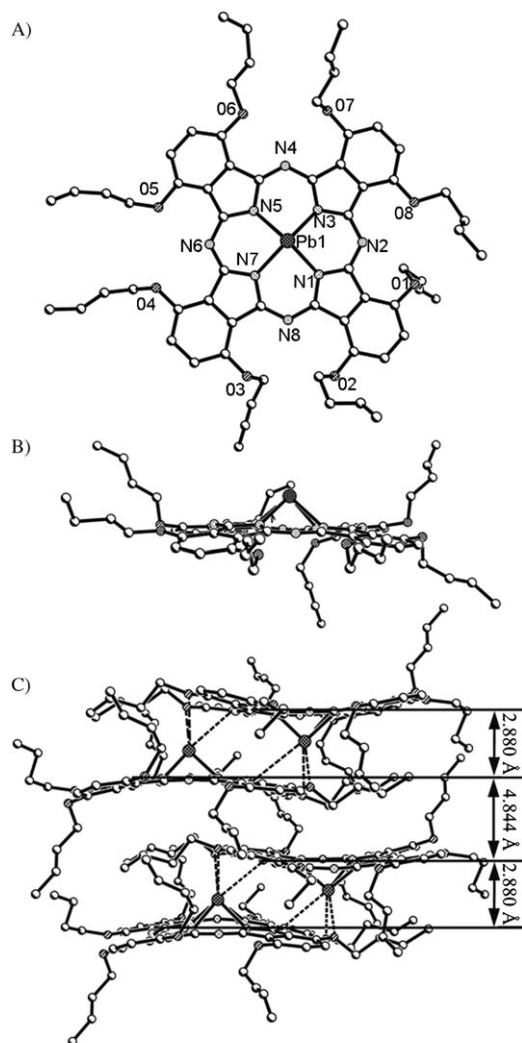


Figure 2. A) Top view and B) side view of the molecular structure of $\text{Pb}[\text{Pc}(\alpha\text{-OC}_4\text{H}_9)_8]$ (**2**) together with C) the Pb-connected pseudo-double-decker supramolecular structures in single crystal of **2** (side view). Hydrogen atoms are omitted for clarity.

revealing the high stability of this Pb-connected pseudo-double-decker supramolecular structure due to the intense π - π interaction between the two phthalocyanine rings. It is worth noting that the short intermolecular distance is a key parameter responsible for the good carrier transfer properties in electronic devices of molecular material.^[53] As detailed below, this Pb-connected pseudo-double-decker supramolecular structure is revealed to be stable enough to exist in the self-assembled nanostructures as basic building blocks according to the XRD data. Similar to the situation in a single crystal of metal-free phthalocyanine **1**, π - π interactions also exist between the neighboring Pb-connected pseudo-double-decker supramolecular structures with a separation of 4.844 Å in terms of the N(isoindole)₄ plane in the crystal of **2** (Figure 2C). It is noteworthy that a similar pseudo-double-decker structure does not exist in the unsubstituted phthalocyaninato lead complex,^[54] thereby indicat-

ing the effect of nonperipheral alkoxy substituents on the molecular arrangement.

In each monomeric unit in the dimeric pseudo-double-decker supramolecular structure, the lead ion is coordinated with four isoindole nitrogen atoms of the phthalocyanine ligand, $\text{Pc}(\alpha\text{-OC}_4\text{H}_9)_8$, in addition to coordinating with one aza-nitrogen atom and two adjacent butyloxy oxygen atoms of the other phthalocyanine ligand. The coordination polyhedron of the lead is thus essentially a slightly distorted polyhedron (Figure S3 in the Supporting Information). However, due to the larger ionic size, the divalent lead ion cannot situate in the central hole of the $\text{Pc}(\alpha\text{-OC}_4\text{H}_9)_8$ but rather sits atop, 1.356 Å above the N(isoindole)₄ plane. As a result, the substituted $\text{Pc}(\alpha\text{-OC}_4\text{H}_9)_8$ ring adopts a conformation that is domed towards the lead cation with $\phi = 9.3^\circ$, which is smaller than that in the corresponding double-decker $\text{EuH}[\text{Pc}(\alpha\text{-OC}_4\text{H}_9)_8]_2$ ($\phi = 16.7^\circ$).^[48]

Electronic absorption spectra: The electronic absorption spectra of the two phthalocyanine derivatives **1** and **2** in CHCl_3 were recorded and the data are compiled in Table 2.

Table 1. Crystallographic data for **1** and **2**.

	1	2
formula	$\text{C}_{64}\text{H}_{82}\text{N}_8\text{O}_8$	$\text{C}_{64}\text{H}_{80}\text{N}_8\text{O}_8\text{Pb}$
M_r	1091.38	1296.55
crystal size [mm ³]	$0.11 \times 0.13 \times 0.15$	$0.13 \times 0.06 \times 0.05$
crystal system	triclinic	monoclinic
space group	$P\bar{1}$	$P21/c$
a [Å]	14.0135(3)	8.2788(13)
b [Å]	14.3092(3)	33.881(5)
c [Å]	16.9072(3)	22.794(4)
α [°]	71.9900(10)	90.00
β [°]	85.8280(10)	99.642(3)
γ [°]	73.4420(10)	90.00
V [Å ³]	3090.01(11)	6303.2(17)
Z	2	4
$F(000)$	1172	2664
ρ_{calcd} [mg m ⁻³]	1.173	1.366
μ [mm ⁻¹]	0.078	0.666
θ range [°]	1.52 to 25.00	1.91 to 23.65
total reflns	32736	27815
independent reflns	10816 ($R_{\text{int}} = 0.0257$)	9464 ($R_{\text{int}} = 0.0663$)
parameters	721	730
$R1$ ($I > 2\sigma(I)$)	0.0791	0.0473
$wR2$ ($I > 2\sigma(I)$)	0.2345	0.1027
GOF	1.024	1.015

As expected, both $\text{H}_2[\text{Pc}(\alpha\text{-OC}_4\text{H}_9)_8]$ (**1**) and $\text{Pb}[\text{Pc}(\alpha\text{-OC}_4\text{H}_9)_8]$ (**2**) show typical features of metal-free and phthalocyaninato metal compounds,^[50,52] respectively, in their electronic absorption spectra, thus revealing their nonaggregated molecular spectroscopic nature in CHCl_3 . As shown in Figure 3, the absorption around 330 nm for **1** can be attributed to the phthalocyanine Soret band, whereas two strong absorptions at 751 and 772 nm with two weak vibronic shoulders around 674 and 703 nm can be attributed to the phthalocyanine Q bands. The weak absorption around 405 nm is common for alkoxy-substituted phthalocyanines,

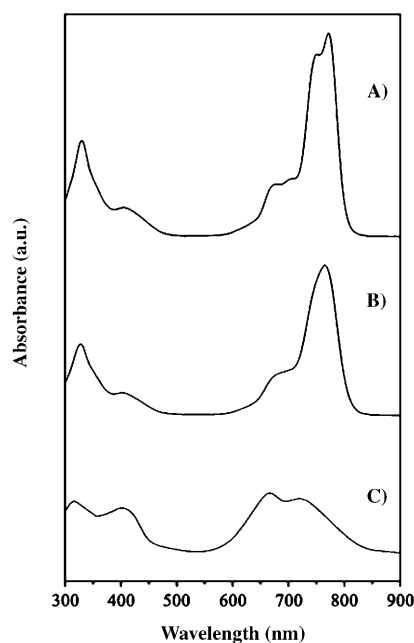


Figure 3. Electronic absorption spectra of A) **1** in CHCl_3 , B) self-assembled aggregates of **1** formed in the absence of Na^+ in methanol, and C) self-assembled aggregates of **1** formed in the presence of Na^+ in methanol.

which is attributed to an $n \rightarrow \pi^*$ transition.^[55] Upon coordination with a lead metal ion, the increase in the molecular symmetry from C_{2h} for **1** to C_{4h} for **2** induces a change in the electronic absorption spectrum from typical features of metal-free phthalocyanine to those typical of phthalocyaninato metal species (Figure S4A in the Supporting Information). The phthalocyanine Soret band is observed at 338 nm and the Q absorption appears at 799 nm as a very strong band with a weak vibronic shoulder at 714 nm for **2** in CHCl_3 . The weak absorption at 472 nm is due to an $n \rightarrow \pi^*$ transition.

The electronic absorption spectra of the aggregates formed from these two phthalocyanine compounds in the absence and presence of Na^+ are also recorded and shown in Figures 3 and S4 (Supporting Information), respectively, which are different from the spectra of corresponding compounds in CHCl_3 . As shown in Figure 3, when the aggregates formed from metal-free phthalocyanine in the absence of Na^+ are dispersed in methanol, the phthalocyanine Soret band at 330 nm in CHCl_3 for metal-free phthalocyanine **1** takes a slight blueshift to 328 nm, and the split phthalocyanine Q bands at 751 and 772 nm change to one weak band and blueshift to 765 nm. Meanwhile, the two weak vibronic bands at 674 and 703 nm also change to one weak absorption and take a blueshift to 676 nm (Table 2). Addition of Na^+ induces further blueshift for the phthalocyanine Q absorption and its vibronic shoulder to 718 and 666 nm, respectively, during the self-assembly process (Table 2), with the phthalocyanine Soret band further blueshifted to 315 nm, thereby revealing the further enhanced intermolecular interaction due to the additionally introduced metal-

ligand ($\text{Na}-\text{N}_{\text{aza}}$ and $\text{Na}-\text{O}_{\text{butyloxy}}$) coordination bonds. This is also true for compound **2** (Figure S4, Supporting Information). On the basis of Kasha's exciton theory,^[56] blueshifts in the main absorption bands of both compounds upon aggregation is typically a sign of the effective $\pi-\pi$ interaction between the phthalocyanine molecules, thus indicating the formation of H aggregates from these two compounds during the self-assembly process both in the absence and presence of Na^+ . Observation of a larger degree of blueshift in the main electronic absorptions for both compounds upon aggregation in the presence of Na^+ indicates stronger intermolecular $\pi-\pi$ interactions than in the aggregates formed in the absence of Na^+ due to the formation of additional metal-ligand ($\text{Na}-\text{N}_{\text{aza}}$ and $\text{Na}-\text{O}_{\text{butyloxy}}$) coordination bonds. This is in good accordance with the XRD analysis results as detailed below.

IR spectrum: The IR spectra of both phthalocyanine derivatives and their self-assembled nanostructures are shown in Figures S5 and S6 in the Supporting Information. The features in the IR spectra of the nanostructures that are similar to that of the corresponding compound for both **1** and **2** unambiguously confirm the composition of nanostructures from corresponding phthalocyanine compounds. The IR spectrum of **1** shows three intense bands at 1598, 1268, and 1038 cm^{-1} due to $\tilde{\nu}(\text{C}=\text{N}-\text{C})$, $\tilde{\nu}_{\text{as}}(\text{C}-\text{O}-\text{C})$, and $\tilde{\nu}_{\text{s}}(\text{C}-\text{O}-\text{C})$, respectively (Figure S5A).^[57] Similar bands were observed at 1597, 1267, and 1037 cm^{-1} in the IR spectrum of aggregates of **1** formed in the absence of Na^+ (Figure S5B). However, as shown in Figure S5C, these three absorptions lose some intensity and appear at 1597, 1265, and 1037 cm^{-1} in the IR spectrum of aggregates of **1** formed in the presence of Na^+ . In particular, two new intensive bands at 865 and 687 cm^{-1} appear in the IR spectrum of the nanostructures of **1** formed in the presence of Na^+ , thereby indicating the formation of $\text{Na}-\text{N}_{\text{aza}}$ and $\text{Na}-\text{O}_{\text{butyloxy}}$ coordination bonds. This is also true for **2** (Figure S6).

Morphology of the aggregates: The morphology of the aggregates formed was examined by scanning electron microscopy (SEM). Samples were prepared by casting a drop of sample solution onto a carbon-coated grid. When injecting a small volume of solution of these two compounds dissolved in CHCl_3 into methanol, nanoribbons with different dimensions were obtained. Depending mainly on the intermolecular $\pi-\pi$ stacking interactions, metal-free molecules of compound **1** in MeOH self-assemble into nanostructures with ribbonlike morphology with uniform size and orientation (Figure 4A). The nanoribbons were ordered over several micrometers with average width of approximately 100 nm, in line with the long range periodicity along (001) and (100) directions as revealed by the XRD analysis. This is also true for **2**. As displayed in Figure 4C, molecules of the phthalocyaninato lead complex **2** also self-assemble into several micrometer-long nanoribbons but with a different average width of approximately 150 nm, thereby revealing the effect of the molecular structure (conformation) on the dimensions

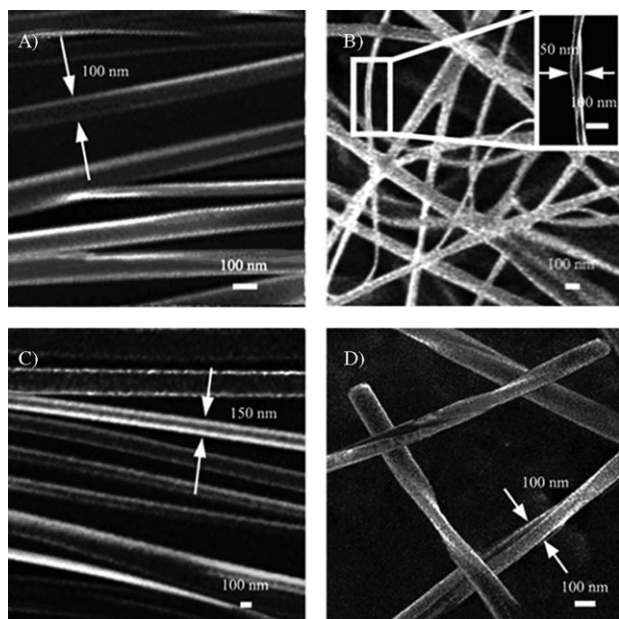


Figure 4. SEM images of nanostructures of **1** and **2**: A) nanoribbons formed from **1** in the absence of Na⁺, B) twisted nanoribbons formed from **1** in the presence of Na⁺, with a magnified image inset, C) nanoribbons formed from **2** in the absence of Na⁺, and D) twisted nanoribbons formed from **2** in the presence of Na⁺ in methanol.

of self-assembled nanostructures. This is also true for the twisted nanoribbons formed from **1** and **2** in the presence of sodium ions.

With the addition of sodium ions, a change in the morphology of self-assembled nanoscale aggregates was revealed, thus showing the effect of additional metal–ligand (Na–N_{aza} and Na–O_{butyloxy}) coordination bonding interactions on the formation of self-assembled nanostructures. As displayed in Figure 4B, molecules of metal-free phthalocyanine **1** self-assemble into nanostructures with a twisted ribbonlike morphology several micrometers in length and with an average width of approximately 50 nm in the presence of Na⁺. A schematic illustration for the formation of twisted nanoribbons in the presence of sodium ions is shown in Figure S7 in the Supporting Information on the basis of the XRD analysis as detailed below. As can be seen in this figure, coordination of two metal-free phthalocyanine molecules with two additionally introduced sodium ions induces the formation of an Na-connected pseudo-double-decker with a twisted structure for the phthalocyanine ligand, which, as a building block, then stacks into the twisted ribbonlike nanostructures depending on intertetrapyrrole π – π interactions. As expected, with the Pb-connected pseudo-double-decker supramolecular structure as building blocks, in the presence of Na⁺ the lead coordination compound **2** also self-assembles into nanostructures with twisted ribbonlike morphology several micrometers in length and with an average width of approximately 100 nm (Figure 4D) due to the formation of additional metal–ligand (Na–N_{aza} and Na–O_{butyloxy}) coordination bonds (Figure S8 in the Supporting Information). It is noteworthy that the left and right orienta-

tions of the twisted nanoribbons formed from both compounds **1** and **2** are generally in the ratio of 1:1 in the whole area of the SEM image as expected.

EDX analysis: To confirm the role of sodium ions in the formation of twisted nanoribbons, energy-dispersive X-ray (EDX) spectroscopy was used to detect the composition of the samples. As displayed in Figure S9A in the Supporting Information, the elemental signature for C, N, O, and Na in the EDX spectrum for the aggregates formed from **1** in the presence of Na⁺ clearly indicates the composition of twisted nanoribbons from metal-free phthalocyanine with the help of sodium ions. This is also true for compound **2**. However, an additional elemental signature for the Pb atom is also observed in the EDX spectrum for the aggregates formed from **2** in the presence of Na⁺ (Figure S9B).

X-ray diffraction patterns of the aggregates: The nanostructures of the two compounds were fabricated by injecting a small volume of solution of **1** and **2** in chloroform (1 mM) into a large volume of methanol in the absence and presence of sodium ions, respectively. Their internal structures were investigated by XRD analysis (Figures 5 and 6; Figure S10 in the Supporting Information). As shown in Figure 5A, in the low-angle range, the XRD diagram of the nanoribbons formed from metal-free phthalocyanine **1** in methanol in the absence of Na⁺ shows three refraction peaks at $2\theta=5.49$ (corresponding to 1.61 nm), 6.57 (1.34 nm), and 7.30° (1.21 nm), respectively, which are unambiguously ascribed to the refractions from the (001), (100), and (011) planes on the basis of simulated powder diffraction patterns of the same compound using Mercury 2.2^[58] according to the X-ray crystallographic data of **1** (Figure 5C; the Miller indices for the simulated powder diffraction pattern of compound **1** are in Table S1 in the Supporting Information). Surprisingly, in the wide-angle range, the XRD pattern presents rich higher order refractions for these three planes at 0.54 (003), 0.40 (004), 0.32 (005), 0.27 (006), 0.23 (007), 0.20 nm (008), 0.67 (200), 0.45 (300), and 0.34 nm (400), and 0.60 (022), 0.40 (033), 0.30 (044), 0.24 nm (055), respectively (Figure 5B), thus revealing the high-molecular-ordering nature of this nanostructure along these directions. Additional refractions at 0.50, 0.48, 0.42, and 0.39 nm were also observed in the wide-angle range of the XRD pattern of the nanoribbons formed from **1** in the absence of Na⁺ and assigned to (10–3), (131), (20–3), and (3–1–1) planes in a confirmed manner on the basis of the simulated powder diffraction pattern (Table S1 in the Supporting Information). Both the peaks at 0.50 and 0.48 nm are assigned to the distance between N(isoindole)₄ planes of neighboring stacking phthalocyanine molecules in the nanoribbons of **1**. This result corresponds well with the alternative separations of 4.961 and 4.848 Å between neighboring phthalocyanine molecules in terms of the N(isoindole)₄ plane revealed in a single crystal of metal-free phthalocyanine. This is also true for the two peaks at 0.40 and 0.34 nm due to the distance between two overlapped isoindole sec-

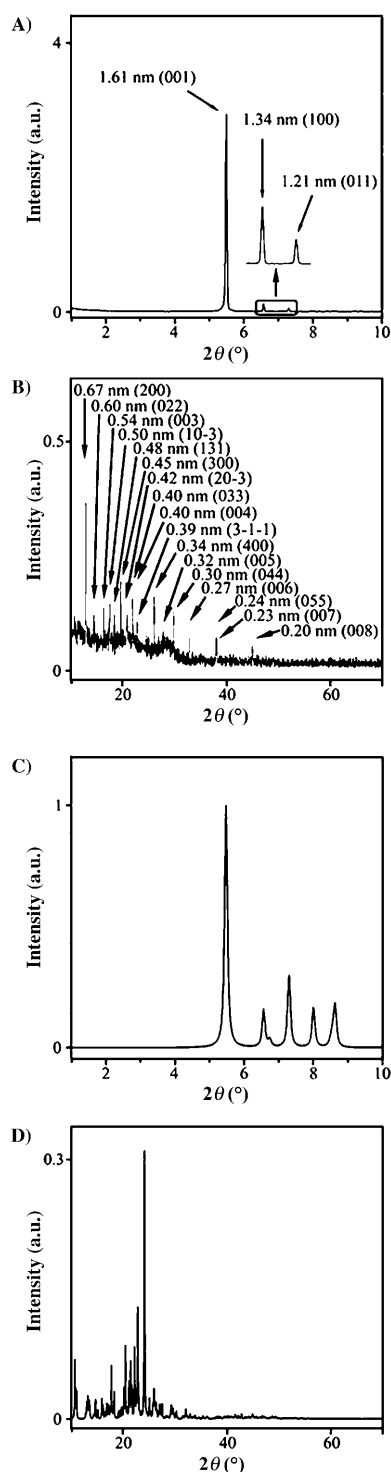


Figure 5. XRD profiles of the nanoribbons formed from **1** in the absence of Na^+ in A) the low-angle range and B) wide-angle range, together with the simulated powder diffraction pattern using Mercury 2.2^[58] on the basis of X-ray crystallographic data in C) the low-angle range and D) wide-angle range.

tions of the neighboring phthalocyanine molecules in the nanoribbons, which is in good accordance with corresponding separations of 3.351 and 4.019 Å revealed in the single crystal. These diffraction results could be assigned to the re-

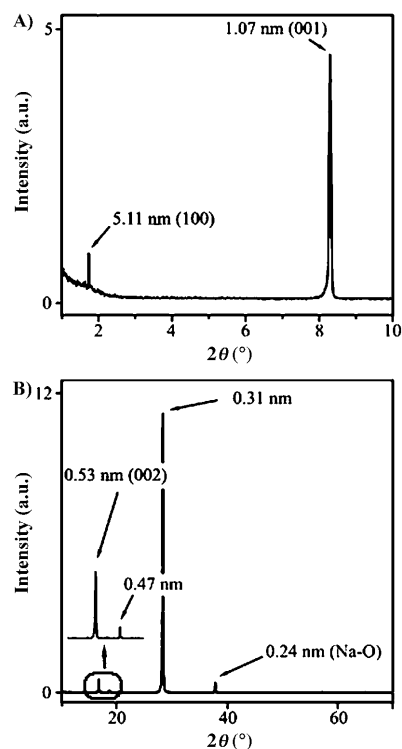


Figure 6. XRD profiles of the twisted nanoribbons formed from **1** in the presence of Na^+ in A) the low-angle range and B) wide-angle range.

fractions from a parallelepipedal lattice (including triclinic system) with cell parameters of $a=1.34$ nm and $c=1.61$ nm, Figure 7. Results comparable to those found for nanoribbons of **1** were revealed for single crystals of the same compound formed in methanol ($a=14.01$ and $c=16.91$ Å;

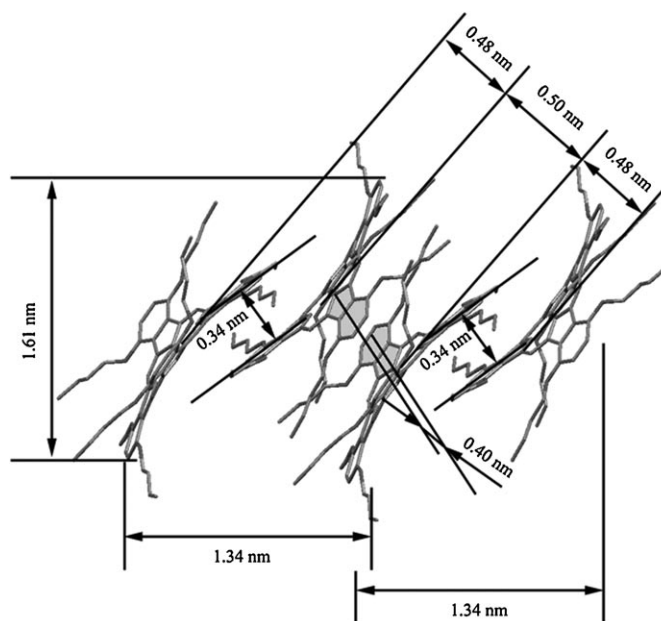


Figure 7. A schematic representation of the unit cell in the nanoribbons formed from **1** in the absence of Na^+ . Hydrogen atoms are omitted for clarity.

Table 1), which suggests their similar molecular packing mode. Further support for this point actually comes from the excellent correspondence in the refraction peaks ob-

shown in Figure 8, during the self-assembly process of **1** in the presence of Na⁺, at the first stage two metal-free phthalocyanine molecules with a saddle conformation coordinate with two sodium ions to form an Na-connected pseudo-double-decker supramolecular structure with a twisted molecular structure for the phthalocyanine ligand, which then acts as the building block for further self-assembly into the twisted nanoribbons, depending mainly

Table 2. Electronic absorption spectral data for **1** and **2** dissolved in CHCl₃ and their aggregates formed in the absence and presence of Na⁺ dispersed in methanol.

	CHCl ₃	λ_{\max} [nm]	
		MeOH (without Na ⁺)	MeOH (with Na ⁺)
1	330, 405, 674, 703, 751, 772	328, 403, 676, 765	315, 401, 666, 718
2	338, 472, 714, 799	333, 467, 704, 781	332, 416, 698, 779

served for the nanoribbons of **1** with those in the simulated powder diffraction pattern of the same compound on the basis of X-ray crystallographic data. As a consequence, metal-free phthalocyanine molecules in the nanoribbons should also pack into a triclinic system with a *P* $\bar{1}$ space group just as in the single crystals. As can be found in the unit cell (Figure S2A in the Supporting Information), due to the saddle molecular conformation employed for **1**, the π - π interaction between neighboring metal-free phthalocyanine molecules actually exists along the *c*-axis direction for two neighboring isoindole sections, the *a*-axis direction also for two neighboring isoindole sections, and the direction perpendicular to the (011) direction for two neighboring N(isoindole)₄ planes, thereby suggesting the advantage of crystal growth along these three directions. This is in good accordance with the observation of a series of higher-order refraction peaks of the (001), (100), and (011) planes in the XRD profile of nanoribbons of **1**. It is worth noting that the lack of the (010) refraction in the XRD diagram of the nanoribbons formed from metal-free phthalocyanine compound **1** in the absence of Na⁺ in methanol indicates the lack of long-range periodicity along this direction in the self-assembled nanostructures. As a result, growth in this direction during the self-assembly process is limited or prohibited, thus resulting in nanoribbons of metal-free phthalocyanine.

As expected, the twisted nanoribbons formed from metal-free phthalocyanine in the presence of Na⁺ show different XRD patterns from those obtained in the absence of Na⁺. As shown in Figure 6, in the low-angle range, the XRD diagram of the twisted nanoribbons of **1** shows two narrow refraction peaks at 5.11 and 1.07 nm, which are ascribed to the refractions from the (100) and (001) planes, respectively. In addition, the XRD pattern also displays four well-defined peaks at 0.53, 0.47, 0.31, and 0.24 nm. The first of these peaks originates from the refraction of the (002) plane, whereas the last one is assigned to the Na-O_{butyloxy} coordination bond length in the nanoribbons (Figure 6).^[47] As clearly

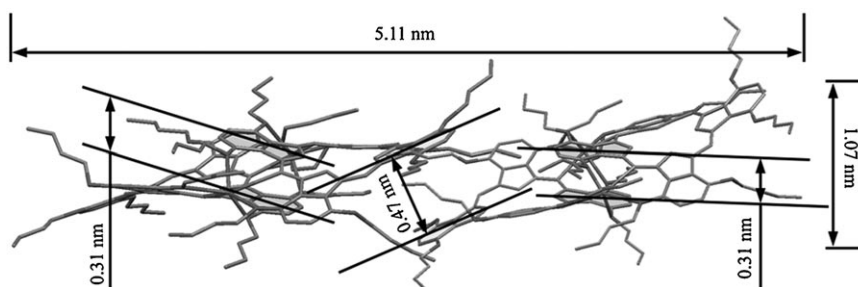


Figure 8. A schematic representation of the unit cell in the twisted nanoribbons formed from **1** in the presence of Na⁺. Hydrogen atoms are omitted for clarity.

on the π - π interactions between two overlapped isoindole sections of neighboring phthalocyanine rings in two neighboring Na-connected pseudo-double-decker building blocks. As we found, the self-assembly behavior of **1** in the presence of Na⁺ is somehow similar to that of the lead complex **2** in the absence of sodium ions except for the twisted phthalocyanine structure in the Na-connected pseudo-double-decker supramolecular structures, thereby resulting in twisted nanoribbons. As detailed above, the further blueshifted absorption bands observed in the electronic absorption spectrum of **1** upon aggregation in the presence of Na⁺ relative to those formed in the absence of Na⁺ gives additional support for the formation of such a pseudo-double-decker supramolecular structure connected by sodium ions through metal-ligand (Na-N_{aza} and Na-O_{butyloxy}) coordination bonds. As a result, the peaks at 0.47 and 0.31 nm for the twisted nanoribbons of **1** attributed to the distance between two overlapped isoindole sections of neighboring phthalocyanine molecules connected with and without sodium ions, respectively, become greater and smaller, respectively, in comparison with those in the single crystals and also in the nanoribbons formed from **1** in the absence of Na⁺ due to the decreased and increased intertetrapyrrole interactions between and within the Na-connected pseudo-double-decker building blocks. According to the above-described XRD diffraction analysis results and the single-crystal molecular structure size of this compound, the unit cell from a parallelepipedal lattice with a cell parameter of *a* = 5.11 and *c* = 1.07 nm is given in Figure 8 for the twisted nanoribbons of **1** formed in the presence of Na⁺.

As shown in Figure S10A in the Supporting Information, in the low-angle range, the XRD profile of the nanoribbons formed from phthalocyaninato lead complex **2** in methanol in the absence of Na^+ shows three strong refraction peaks at 1.90, 1.65, and 1.59 nm, respectively, which are attributed to the (100), (001), and (010) planes due to the observation of rich higher refraction peaks for the former two peaks. The remaining weak refraction at 0.94 nm (200) in the low-angle range is due to the second-order refraction peak of the (100) plane. In the wide-angle range of the XRD pattern, the three basic (001), (100), and (010) planes give their higher-order refractions at 0.84 (002), 0.54 (003), 0.42 (004), 0.32 nm (005); 0.62 nm (300); and 0.40 nm (040), respectively. Observation of a series of higher-order refraction peaks of the (001) plane suggests the advantage of crystal growth along this direction, thereby resulting in nanostructures with a ribbonlike morphology for this phthalocyaninato lead complex. On the basis of these XRD diffraction analysis results and the single-crystal molecular structure of this compound, the unit cell consisting of two Pb-connected pseudo-double-decker building blocks (four phthalocyaninato lead molecules) from a parallelepipedal lattice (including a monoclinic system) with the cell parameters of $a = 1.90$, $b = 1.59$, and $c = 1.65$ nm is given in Figure S11 in the Supporting Information for the nanoribbons of **2**. Comparison between this unit cell of the nanoribbons for **2** and that revealed for single crystals of the same compound also formed in methanol reveals their different molecular packing mode (Table 1), thereby indicating the effect of crystal growth speed on the system and dimensions of the crystal unit cell for this compound. In addition, as clearly shown in the unit cell of the single crystals of **2** (Figure S2B in the Supporting Information), an intertetrapyrrole π - π interaction exists in the single crystal along the a -axis direction. However, as detailed above, the advantageous growth direction in the nanoribbons of the same compound formed in the absence of Na^+ is along the c axis. The two remaining sharp refraction peaks at 0.50 and 0.29 nm observed for the nanoribbons of **2** in the wide-angle region are assigned to the stacking distance between the $\text{N}(\text{isoindole})_4$ plane of neighboring phthalocyanine molecules between and within the Pb-connected pseudo-double-deckers, respectively, which corresponds well with those revealed in a single crystal of **2**, 4.844 and 2.880 Å.

The XRD pattern of twisted nanoribbons self-assembled from **2** in the presence of Na^+ shows two peaks at 1.20 and 1.08 nm in the low-angle region, which are ascribed to the refractions from the (100) and (001) planes, respectively (Figure S10B in the Supporting Information).^[45] In the wide-angle region, the XRD pattern also presents four sharp peaks at 0.53, 0.36, 0.27, and 0.21 nm due to the refractions from the (00 l) planes with $l = 2, 3, 4,$ and 5 . The two additional peaks at 0.42 and 0.28 are assigned to the refractions from the stacking distance between the $\text{N}(\text{isoindole})_4$ plane of neighboring phthalocyanine molecules between and within the Pb-connected pseudo-double-deckers, respectively (Figure S12). Both of these, in particular the distance be-

tween the Pb-connected pseudo-double-deckers, become significant shorter than those in the nanoribbons of the same compound formed in the absence of Na^+ , thereby revealing the further enhanced intertetrapyrrole interaction between Pb-connected pseudo-double-deckers due to the formation of additional metal-ligand (Na-N_{aza} and $\text{Na-O}_{\text{butyloxy}}$) coordination bonds. In line with the twisted nanoribbons of **1**, the remaining refraction at 0.24 nm is clearly due to the Na-O coordination bond length in the twisted nanoribbons of **2**.

Conclusion

In the present paper, two nonperipherally octa(alkoxyl)-substituted phthalocyanine compounds, **1** and **2**, with good crystallinity were synthesized. Their self-assembly behavior in the absence and presence of sodium ions has been comparatively studied. Intermolecular π - π interactions between the metal-free phthalocyanine molecules with a saddle molecular conformation for **1** and Pb-connected pseudo-double-decker supramolecular building blocks with a domed molecular conformation for the phthalocyanine ligand for **2** led to the formation of nanoribbons with an average width of approximately 100 and 150 nm, respectively, thereby revealing the effect of molecular structure (conformation) on the dimensions of the self-assembled nanostructures.

In the presence of sodium ions, the formation of additional metal-ligand (Na-N_{aza} and $\text{Na-O}_{\text{butyloxy}}$) coordination bonds between sodium atoms and aza-nitrogen atoms and the adjacent butyloxy oxygen atoms of two metal-free phthalocyanine molecules in cooperation with the intrinsic intermolecular π - π interaction induces the formation of Na-connected pseudo-double-decker building blocks, which then self-assemble into twisted nanoribbons with an average width of approximately 50 nm depending on the intertetrapyrrole π - π interaction. Twisted nanoribbons with an average width of approximately 100 nm were also formed from **2** with Pb-connected pseudo-double-decker supramolecular structures as building blocks depending on the combination of metal-ligand (Na-N_{aza} and $\text{Na-O}_{\text{butyloxy}}$) coordination bonding interactions with intrinsic intertetrapyrrole π - π interactions. In particular, both nanoribbons and twisted nanoribbons display rich refraction peaks in their X-ray diffraction patterns, thus revealing the high molecular ordering nature of these nanostructures. To the best of our knowledge, the present result represents the first self-assembled nanostructures fabricated from phthalocyanine derivatives with a confirmed internal structure, controllable dimensions, and high molecular ordering nature. It will be helpful for the design and preparation of phthalocyanine-based nanoelectronic and nano-optoelectronic devices with good performance due to the close relationship between the molecular ordering and dimensions of nanostructures and the performance and size of nanodevices.

Experimental Section

Measurements: The nanostructures of compounds **1** and **2** were fabricated by using the phase-transfer method according to the following procedure.^[25,31c,59–61] A minimum volume (30–50 μL) of a concentrated solution of **1** (or **2**) (1 mM) in chloroform was injected rapidly into a large volume of methanol or methanol containing saturated sodium hydroxide (1 mL) and subsequently mixed with a microinjector. The results were reproducible under the experimental conditions described above. ^1H NMR spectra were recorded using a Bruker DPX 300 spectrometer (300 MHz) in CDCl_3 using the residual solvent resonance of CHCl_3 at $\delta = 7.26$ ppm relative to SiMe_4 as internal reference. Electronic absorption spectra were recorded using a Hitachi U-4100 spectrophotometer. X-ray diffraction experiments were carried out using a Rigaku D/max- γB X-ray diffractometer. MALDI-TOF mass spectra were recorded using a Bruker BIFLEX III ultra-high resolution Fourier transform ion cyclotron resonance (FTICR) mass spectrometer with α -cyano-4-hydroxycinnamic acid as the matrix. Elemental analyses were performed by the Institute of Chemistry, Chinese Academy of Sciences. SEM images were obtained using a JEOL JSM-6700F field-emission scanning electron microscope. For SEM imaging, Au (1–2 nm) was sputtered onto the grids to prevent charging effects and to improve the image clarity.

Chemicals: Column chromatography was carried out on silica gel (Merck, Kieselgel 60, 70–230 mesh) with the indicated eluents. All other reagents and solvents were used as received.

Preparation of $\text{Pb}[\text{Pc}(\alpha\text{-OC}_4\text{H}_9)_8]$ (2**):** In a typical procedure, a mixture of 1,4,8,11,15,18,22,25-octa(butyloxy)phthalocyanine (109 mg, 0.10 mmol) and $\text{Pb}(\text{OAc})_2 \cdot 3\text{H}_2\text{O}$ (76 mg, ca. 0.20 mmol) in DMF (4 mL) was heated to reflux under nitrogen for approximately 5 h. The solvent was then removed in vacuo, and the residue was subjected to chromatography on a silica gel column using CHCl_3 as eluent. The crude product was purified by recrystallization from $\text{CHCl}_3/\text{MeOH}$, giving a dark green compound (118 mg, 91.0%). ^1H NMR (CDCl_3 , 300 MHz): $\delta = 7.57$ (s, 8H; $\text{Pc}(\alpha\text{-OC}_4\text{H}_9)_8$ H_β), 4.81–4.87 (t, 16H; $\text{OCH}_2\text{C}_3\text{H}_7$), 2.18–2.26 (m, 16H; $\text{OCH}_2\text{CH}_2\text{C}_2\text{H}_5$), 1.59–1.69 (m, 16H; $\text{OC}_2\text{H}_4\text{CH}_2\text{CH}_3$), 1.05–1.10 ppm (t, 24H; $\text{OC}_2\text{H}_4\text{CH}_3$). MALDI-TOF MS (with an isotopic cluster peaking at 1297.6); m/z : calcd for $\text{C}_{64}\text{H}_{80}\text{N}_8\text{O}_8\text{Pb}$ $[M+H]^+$: 1297.6; elemental analysis calcd (%) for $\text{C}_{64}\text{H}_{80}\text{N}_8\text{O}_8\text{Pb}$: C 59.29, H 6.22, N 8.64; found: C 59.16, H 5.37, N 8.71.

X-ray crystallographic analyses of **1 and **2**:** Crystal data and details of data collection and structure refinement are given in Table 1. Data were collected using a Bruker SMART CCD diffractometer with an $\text{MoK}\alpha$ sealed tube ($\lambda = 0.71073$ Å) at 293 K, using a ω scan mode with an increment of 0.3° . Preliminary unit-cell parameters were obtained from 45 frames. Final unit-cell parameters were obtained by global refinements of reflections obtained from integration of all the frame data. The collected frames were integrated using the preliminary cell-orientation matrix. The SMART software was used for collecting frames of data, indexing reflections, and determination of lattice constants; SAINT-PLUS for integration of intensity of reflections and scaling;^[62] SADABS for absorption correction;^[63] and SHELXL for space group and structure determination, refinements, graphics, and structure reporting.^[64]

CCDC-720293 (**1**) and -733416 (**2**) contain the supplementary crystallographic data for this paper. These data can be obtained free of charge from The Cambridge Crystallographic Data Centre via www.ccdc.cam.ac.uk/data_request/cif.

Acknowledgements

Financial support from the Natural Science Foundation of China (Grant No. 20931001) and the Ministry of Education of China is gratefully acknowledged.

[1] M. J. Bierman, Y. K. A. Lau, A. V. Kvit, A. L. Schmitt, S. Jin, *Science* **2008**, *320*, 1060–1063.

- [2] L. Zang, Y. Che, J. S. Moore, *Acc. Chem. Res.* **2008**, *41*, 1596–1608.
 [3] X. Wang, Q. Peng, Y. Li, *Acc. Chem. Res.* **2007**, *40*, 635–643.
 [4] T. Shimizu, M. Masuda, H. Minamikawa, *Chem. Rev.* **2005**, *105*, 1401–1443.
 [5] G.-Y. Liu, S. Xu, Y. Qian, *Acc. Chem. Res.* **2000**, *33*, 457–466.
 [6] a) A. M. Shultz, O. K. Farha, J. T. Hupp, S. T. Nguyen, *J. Am. Chem. Soc.* **2009**, *131*, 4204–4205; b) S. J. Lee, S.-H. Cho, K. L. Mulfort, D. M. Tiede, J. T. Hupp, S. T. Nguyen, *J. Am. Chem. Soc.* **2008**, *130*, 16828–16829.
 [7] G. M. Whitesides, M. Boncheva, *Proc. Natl. Acad. Sci. USA* **2002**, *99*, 4769–4774.
 [8] B. Olenyuk, J. A. Whiteford, A. Fechtenkotter, P. J. Stang, *Nature* **1999**, *398*, 796–799.
 [9] I. C. Reynhout, J. J. L. M. Cornelissen, R. J. M. Nolte, *Acc. Chem. Res.* **2009**, *42*, 681–692.
 [10] a) M. Kimura, Y. Saito, K. Ohta, K. Hanabusa, H. Shirai, N. Kobayashi, *J. Am. Chem. Soc.* **2002**, *124*, 5274–5275; b) M. Kimura, K. Wada, K. Ohta, K. Hanabusa, H. Shirai, N. Kobayashi, *Macromolecules* **2001**, *34*, 4706–4711.
 [11] a) M. Kimura, H. Ueki, K. Ohta, K. Hanabusa, H. Shirai, N. Kobayashi, *Langmuir* **2002**, *18*, 7683–7687; b) M. Kimura, W. Kazumi, K. Ohta, K. Hanabusa, H. Shirai, N. Kobayashi, *J. Am. Chem. Soc.* **2001**, *123*, 2438–2439; c) M. Kimura, T. Muto, H. Takimoto, W. Kazumi, K. Ohta, K. Hanabusa, H. Shirai, N. Kobayashi, *Langmuir* **2000**, *16*, 2078–2082.
 [12] a) J. D. Hartgerink, E. Beniash, S. I. Stupp, *Science* **2001**, *294*, 1684–1688; b) T. Kitamura, S. Nakaso, N. Mizoshita, Y. Tochigi, T. Shimomura, M. Moriyama, K. Ito, T. Kato, *J. Am. Chem. Soc.* **2005**, *127*, 14769–14775.
 [13] A. D. Schwab, D. E. Smith, B. Bond-Watts, D. E. Johnston, J. Hone, A. T. Johnson, J. C. de Paula, W. F. Smith, *Nano. Lett.* **2004**, *4*, 1261–1265.
 [14] Z. Wang, Z. Li, C. J. Medforth, J. A. Shelnutt, *J. Am. Chem. Soc.* **2007**, *129*, 2440–2441.
 [15] a) D. Y. Yan, Y. F. Zhou, J. Hou, *Science* **2004**, *303*, 65–67; b) T. Shimizu, M. Masuda, H. Minamikawa, *Chem. Rev.* **2005**, *105*, 1401–1444; c) L. Zhi, T. Gorelik, J. Wu, U. Kolb, K. Müllen, *J. Am. Chem. Soc.* **2005**, *127*, 12792–12793; d) J.-S. Hu, Y.-G. Guo, H.-P. Liang, L.-J. Wan, L. Jiang, *J. Am. Chem. Soc.* **2005**, *127*, 17090–17095.
 [16] P. H. Dinolfo, J. T. Hupp, *Chem. Mater.* **2001**, *13*, 3113–3125.
 [17] E. Hao, K. L. Kelly, J. T. Hupp, G. C. Schatz, *J. Am. Chem. Soc.* **2002**, *124*, 15182–15183.
 [18] a) Y. Guo, Q. Tang, H. Liu, Y. Zhang, Y. Li, W. Hu, S. Wang, D. Zhu, *J. Am. Chem. Soc.* **2008**, *130*, 9198–9199; b) Y. Guo, Y. Li, J. Xu, X. Liu, J. Xu, J. Lv, C. Huang, M. Zhu, S. Cui, L. Jiang, H. Liu, S. Wang, *J. Phys. Chem. C* **2008**, *112*, 8223–8228.
 [19] a) Y. Zhou, W. Liu, Y. Ma, H. Wang, L. Qi, Y. Cao, J. Wang, J. Pei, *J. Am. Chem. Soc.* **2007**, *129*, 12386–12387; b) L. Wang, Y. Zhou, J. Yan, J. Wang, J. Pei, Y. Cao, *Langmuir* **2009**, *25*, 1306–1310.
 [20] T. Kishida, N. Fujita, K. Sada, S. Shinkai, *J. Am. Chem. Soc.* **2005**, *127*, 7298–7299.
 [21] a) H. Liu, Y. Li, S. Xiao, H. Gan, T. Jiu, H. Li, L. Jiang, D. Zhu, D. Yu, B. Xiang, Y. Chen, *J. Am. Chem. Soc.* **2003**, *125*, 10794–10795; b) M. Enomoto, A. Kishimura, T. Aida, *J. Am. Chem. Soc.* **2001**, *123*, 5608–5609; c) H.-B. Chen, Y. Zhou, J. Yin, J. Yan, Y. Ma, L. Wang, Y. Cao, J. Wang, J. Pei, *Langmuir* **2009**, *25*, 5459–5462.
 [22] a) G. Lu, Y. Chen, Y. Zhang, M. Bao, Y. Bian, X. Li, J. Jiang, *J. Am. Chem. Soc.* **2008**, *130*, 11623–11630; b) Y. Gao, X. Zhang, C. Ma, X. Li, J. Jiang, *J. Am. Chem. Soc.* **2008**, *130*, 17044–17052.
 [23] a) M. Shirakawa, N. Fujita, S. Shinkai, *J. Am. Chem. Soc.* **2003**, *125*, 9902–9903; b) S. Tanaka, M. Shirakawa, K. Kaneko, M. Takeuchi, S. Shinkai, *Langmuir* **2005**, *21*, 2163–2172.
 [24] a) M. Shirakawa, N. Fujita, S. Shinkai, *J. Am. Chem. Soc.* **2005**, *127*, 4164–4165; b) S. J. Lee, J. T. Hupp, S. T. Nguyen, *J. Am. Chem. Soc.* **2008**, *130*, 9632–9633.
 [25] a) K. Balakrishnan, A. Datar, T. Naddo, J. Huang, R. Oitker, M. Yen, J. Zhao, L. Zang, *J. Am. Chem. Soc.* **2006**, *128*, 7390–7398; b) Y. Che, A. Datar, K. Balakrishnan, Z. Ling, *J. Am. Chem. Soc.* **2007**, *129*, 7234–7235.

- [26] a) J. Luo, T. Lei, L. Wang, Y. Ma, Y. Cao, J. Wang, J. Pei, *J. Am. Chem. Soc.* **2009**, *131*, 2076–2077; b) H. Gan, H. Liu, Y. Li, Q. Zhao, Y. Li, S. Wang, T. Jiu, N. Wang, X. He, D. Yu, D. Zhu, *J. Am. Chem. Soc.* **2005**, *127*, 12452–12453.
- [27] H. Liu, Q. Zhao, Y. Li, Y. Liu, F. Lu, J. Zhuang, S. Wang, L. Jiang, D. Zhu, D. Yu, L. Chi, *J. Am. Chem. Soc.* **2005**, *127*, 1120–1121.
- [28] a) T. Yamaguchi, N. Ishii, K. Tashiro, T. Aida, *J. Am. Chem. Soc.* **2003**, *125*, 13934–13935; b) A. Tsuda, S. Sakamoto, K. Yamaguchi, T. Aida, *J. Am. Chem. Soc.* **2003**, *125*, 15722–15723; c) Y. Guo, H. Oike, T. Aida, *J. Am. Chem. Soc.* **2004**, *126*, 716–717.
- [29] a) H. Liu, Y. Li, L. Jiang, H. Luo, S. Xiao, H. Fang, H. Li, D. Zhu, D. Yu, J. Xu, B. Xiang, *J. Am. Chem. Soc.* **2002**, *124*, 13370–13371; b) W. Lv, X. Zhang, J. Lu, Y. Zhang, X. Li, J. Jiang, *Eur. J. Inorg. Chem.* **2008**, 4255–4261.
- [30] a) J. Motoyanagi, T. Fukushima, N. Ishii, T. Aida, *J. Am. Chem. Soc.* **2006**, *128*, 4220–4221; b) W.-S. Li, K. S. Kim, D.-L. Jiang, H. Tanaka, T. Kawai, J. H. Kwon, D. Kim, T. Aida, *J. Am. Chem. Soc.* **2006**, *128*, 10527–10532; c) T. Yamamoto, T. Fukushima, Y. Yamamoto, A. Kosaka, W. Jin, N. Ishii, T. Aida, *J. Am. Chem. Soc.* **2006**, *128*, 14337–14340; d) Y. Yamamoto, T. Fukushima, A. Saeiki, S. Seki, S. Tagawa, N. Ishii, T. Aida, *J. Am. Chem. Soc.* **2007**, *129*, 9276–9277; e) J. L. Mynar, T. Yamamoto, A. Kosaka, T. Fukushima, N. Ishii, T. Aida, *J. Am. Chem. Soc.* **2008**, *130*, 1530–1531.
- [31] a) A. B. P. Lever, C. C. Leznoff, *Phthalocyanine: Properties and Applications, Vols. 1–4*, VCH, Weinheim, **1989–1996**; b) N. B. McKeown, *Phthalocyanines Materials: Synthesis Structure and Function*, Cambridge University Press, New York, **1998**; c) K. M. Kadish, K. M. Smith, R. Guilard, *The Porphyrin Handbook, Vols. 1–20*, Academic Press, San Diego, **2000–2003**.
- [32] a) J. A. de Saja, M. L. Rodríguez-Méndez, *Adv. Colloid Interface Sci.* **2005**, *116*, 1–11; b) V. Parra, M. Bouvet, J. Brunet, M. L. Rodríguez-Méndez, J. A. de Saja, *Thin Solid Films* **2008**, *516*, 9012–9019; c) V. Parra, J. Brunet, A. Pauly, M. Bouvet, *Analyst* **2009**, *9*, 1776–1778.
- [33] a) J. Jiang, D. K. P. Ng, *Acc. Chem. Res.* **2009**, *42*, 79–88; b) J. Jiang, W. Liu, D. P. Arnold, *J. Porphyrins Phthalocyanines* **2003**, *7*, 459–473; c) J. Jiang, K. Kasuga, D. P. Arnold in *Supramolecular Photosensitive and Electro-active Materials* (Ed.: H. S. Nalwa), Academic Press, New York, **2001**, pp. 113–210; d) D. K. P. Ng, J. Jiang, *Chem. Soc. Rev.* **1997**, *26*, 433–442.
- [34] a) J. Simon, J. Andre, *Molecular Semiconductors*, Springer, Berlin, **1985**; b) M. Bouvet, J. Simon, *Chem. Phys. Lett.* **1990**, *172*, 299–302; c) Y. Chen, W. Su, M. Bai, J. Jiang, X. Li, Y. Liu, L. Wang, S. Wang, *J. Am. Chem. Soc.* **2005**, *127*, 15700–15701; d) Y. Gao, P. Ma, Y. Chen, Y. Zhang, Y. Bian, X. Li, J. Jiang, C. Ma, *Inorg. Chem.* **2009**, *48*, 45–54; e) R. Li, P. Ma, S. Dong, X. Zhang, Y. Chen, X. Li, J. Jiang, *Inorg. Chem.* **2007**, *46*, 11397–11404; f) Y. Chen, R. Li, R. Wang, P. Ma, S. Dong, Y. Gao, X. Li, J. Jiang, *Langmuir* **2007**, *23*, 12549–12554.
- [35] Z. Liu, A. A. Yasser, J. S. Lindsey, D. F. Bocian, *Science* **2003**, *302*, 1543–1545.
- [36] a) N. Ishikawa, M. Sugita, W. Wernsdorfer, *Angew. Chem.* **2005**, *117*, 2991; *Angew. Chem. Int. Ed.* **2005**, *44*, 2931–2935; b) N. Ishikawa, M. Sugita, W. Wernsdorfer, *J. Am. Chem. Soc.* **2005**, *127*, 3650–3651; c) N. Ishikawa, M. Sugita, T. Ishikawa, S.-y. Koshihara, Y. Kaizu, *J. Am. Chem. Soc.* **2003**, *125*, 8694–8695.
- [37] D. J. Hill, M. J. Mio, R. B. Prince, T. S. Hughes, J. S. Moore, *Chem. Rev.* **2001**, *101*, 3893–4012.
- [38] J.-M. Lehn, *Supramolecular Chemistry*, VCH, Weinheim, **1995**.
- [39] J. A. A. W. Elemans, R. van Hameren, R. J. M. Nolte, A. E. Rowan, *Adv. Mater.* **2006**, *18*, 1251–1226.
- [40] a) Z. Shi, Y. Li, H. Gong, M. Liu, S. Xiao, H. Liu, H. Li, S. Xiao, D. Zhu, *Org. Lett.* **2002**, *4*, 1179–1182; b) Y. Li, N. Wang, H. Gan, H. Liu, H. Li, Y. Li, X. He, C. Huang, S. Cui, S. Wang, D. Zhu, *J. Org. Chem.* **2005**, *70*, 9686–9692; c) H. Gan, Y. Li, H. Liu, S. Wang, C. Li, M. Yuan, X. Liu, C. Wang, L. Jiang, D. Zhu, *Biomacromolecules* **2007**, *8*, 1723–1729.
- [41] W. Y. Tong, A. B. Djurii, M. H. Xie, A. C. M. Ng, K. Y. Cheung, W. K. Chan, Y. H. Leung, H. W. Lin, S. Gwo, *J. Phys. Chem. B* **2006**, *110*, 17406–17413.
- [42] V. Duzhko, K. D. Singer, *J. Phys. Chem. C* **2007**, *111*, 27–31.
- [43] C. F. van Nostrum, S. J. Picken, A.-J. Schouten, R. J. M. Nolte, *J. Am. Chem. Soc.* **1995**, *117*, 9957–9965.
- [44] a) M. J. Cook, J. McMurdo, D. A. Miles, R. H. Poynter, J. M. Simmons, S. D. Haslam, R. M. Richardson, K. Wellford, *J. Mater. Chem.* **1994**, *4*, 1205–1213; b) M. J. Cook, *J. Mater. Sci.: Mater. Electron.* **1994**, *5*, 117–128.
- [45] Y. Zhang, Z. Zhang, Y. Zhao, Y. Fan, T. Tong, H. Zhang, Y. Wang, *Langmuir* **2009**, *25*, 6045–6048.
- [46] a) M. J. Cook, J. McMurdo, A. K. Powell, *Chem. Commun.* **1993**, 903–904; b) M. P. Donzello, C. Ercolani, A. A. Gaberkorn, E. V. Kudrik, M. Meneghetti, G. Marcolongo, C. Rizzoli, P. A. Stuzhin, *Chem. Eur. J.* **2003**, *9*, 4009–4024; c) N. B. McKeown, H. Li, M. Hel-iwell, *J. Porphyrins Phthalocyanines* **2005**, *9*, 841–845.
- [47] H. Zhang, R. Wang, P. Zhu, Z. Lai, J. Han, C.-F. Choi, D. K. P. Ng, X. Cui, C. Ma, J. Jiang, *Inorg. Chem.* **2004**, *43*, 4740–4742.
- [48] Y. Gao, R. Li, S. Dong, Y. Bian, J. Jiang, *Dalton Trans.* in press.
- [49] M. J. Cook, A. J. Dunn, S. D. Howe, A. J. Thomson, K. J. Harrison, *J. Chem. Soc. Perkin Trans. 1* **1988**, 2453–2458.
- [50] R. Li, X. Zhang, P. Zhu, D. K. P. Ng, N. Kobayashi, J. Jiang, *Inorg. Chem.* **2006**, *45*, 2327–2334.
- [51] P. M. Burnham, M. J. Cook, L. A. Gerrard, M. J. Heeney, D. L. Hughes, *Chem. Commun.* **2003**, 2064–2065.
- [52] Y. Bian, L. Li, J. Dou, D. Y. Y. Cheng, R. Li, C. Ma, D. K. P. Ng, N. Kobayashi, J. Jiang, *Inorg. Chem.* **2004**, *43*, 7539–7544.
- [53] a) M. Bouvet, E. Silinsh, J. Simon, *Mol. Cryst. Liq. Cryst.* **1995**, *5*, 255–277; b) M. Bouvet in *The Porphyrin Handbook, Vol. 19* (Eds.: K. Kadish, K. M. Smith, R. Guilard), Academic Press, San Diego, **2003**, pp. 37–104.
- [54] a) K. Ukei, *Acta Crystallogr. Sect. B* **1973**, *29*, 2290–2292; b) F. Przyborowski, C. Hamann, *Cryst. Res. Technol.* **1982**, *17*, 1041–1045; c) Y. Iyechika, K. Yakushi, I. Ikemoto, H. Kuroda, *Acta Crystallogr. Sect. B* **1982**, *38*, 766–770.
- [55] a) Y. Zhang, X. Zhang, Z. Liu, Y. Bian, J. Jiang, *J. Phys. Chem. A* **2005**, *109*, 6363–6370; b) N. Sheng, R. Li, C.-F. Choi, W. Su, D. K. P. Ng, X. Cui, K. Yoshida, N. Kobayashi, J. Jiang, *Inorg. Chem.* **2006**, *45*, 3794–3802.
- [56] M. Kasha, H. R. Rawls, M. A. EL-Bayoumi, *Pure Appl. Chem.* **1965**, *11*, 371–392.
- [57] J. Jiang, M. Bao, L. Rintoul, D. P. Arnold, *Coord. Chem. Rev.* **2006**, *250*, 424–448.
- [58] a) C. F. Macrae, I. J. Bruno, J. A. Chisholm, P. R. Edgington, P. McCabe, E. Pidcock, L. Rodriguez-Monge, R. Taylor, J. van de S-treek, P. A. Wood, *J. Appl. Crystallogr.* **2008**, *41*, 466–470; b) C. F. Macrae, P. R. Edgington, P. McCabe, E. Pidcock, G. P. Shields, R. Taylor, M. Towler, J. van de S-treek, *J. Appl. Crystallogr.* **2006**, *39*, 453–457; c) I. J. Bruno, J. C. Cole, P. R. Edgington, M. K. Kessler, C. F. Macrae, P. McCabe, J. Pearson, R. Taylor, *Acta Crystallogr. Sect. B* **2002**, *58*, 389–397; d) R. Taylor, C. F. Macrae, *Acta Crystallogr. Sect. B* **2001**, *57*, 815–827.
- [59] B. A. Minch, W. Xia, C. L. Donley, R. M. Hernandez, C. Carter, M. D. Carducci, A. Dawson, D. F. O'Brien, N. R. Armstrong, *Chem. Mater.* **2005**, *17*, 1618–1627.
- [60] a) I. Hamza, *ACS Chem. Biol.* **2006**, *1*, 627–629; b) P.-C. Lo, C. M. H. Chan, J.-Y. Liu, W.-P. Fong, D. K. P. Ng, *J. Med. Chem.* **2007**, *50*, 2100–2107; c) R. Vanyúr, K. Héberger, J. Jakus, *J. Chem. Inf. Comput. Sci.* **2003**, *43*, 1829–1836.
- [61] a) H. Kasai, H. S. Nalwa, H. Oikawa, S. Okada, H. Matsuda, N. Minami, A. Kakuta, K. Ono, A. Mukoh, H. Nakanishi, *Jpn. J. Appl. Phys.* **1992**, *31*, L1132–L1134; b) F. Bertorelle, D. Lavabre, S. Fery-Forgues, *J. Am. Chem. Soc.* **2003**, *125*, 6244–6253; c) H. Fu, D. Xiao, J. Yao, G. Yang, *Angew. Chem.* **2003**, *115*, 2989–2992; *Angew. Chem. Int. Ed.* **2003**, *42*, 2883–2886; d) S. J. Lee, R. A. Jensen, C. D. Malliakas, M. G. Kanatzidis, J. T. Hupp, S. T. Nguyen, *J. Mater. Chem.* **2008**, *18*, 3640–3642; e) S. J. Lee, C. D. Malliakas, M. G. Kanatzidis, J. T. Hupp, S. T. Nguyen, *Adv. Mater.* **2008**, *20*, 3543–3549;

- f) G. Lu, X. Zhang, X. Cai, J. Jiang, *J. Mater. Chem.* **2009**, *19*, 2417–2424.
- [62] SMART and SAINT for Windows NT Software Reference Manuals, Version 5.0, Bruker Analytical X-Ray Systems, Madison WI, **1997**.
- [63] SADABS, A Software for Empirical Absorption Correction, G. M. Sheldrick, University of Göttingen, Göttingen, **1997**.
- [64] SHELXL Reference Manual, Version 5.1, Bruker Analytical X-Ray Systems, Madison WI, **1997**.

Received: June 23, 2009
Revised: August 22, 2009
Published online: October 28, 2009